Structure and function of bark and wood chloroplasts in a drought-tolerant tree (*Fraxinus ornus* L.)

Sara Natale [1,3], Nicoletta La Rocca[2], Mariano Battistuzzi [2], Tomas Morosinotto[2], Andrea Nardini [1] and Alessandro Alboresi[2]

[1]Department of Life Sciences, University of Trieste, Via L. Giorgieri 10, Trieste 34127, Italy; [2]Department of Biology, University of Padova, Via Ugo Bassi 58B, Padova 35121, Italy; [3]Corresponding author (sara.natale@phd.units.it)

Leaves are the most important photosynthetic organs in most woody plants, but chloroplasts are also found in organs optimized for other functions. However, the actual photosynthetic efficiency of these chloroplasts is still unclear. We analyzed bark and wood chloroplasts of *Fraxinus ornus* L. saplings. Optical and spectroscopic methods were applied to stem samples and compared with leaves. A sharp light gradient was detected along the stem radial direction, with blue light mainly absorbed by the outer bark, and far-red-enriched light reaching the underlying xylem and pith. Chlorophylls were evident in the xylem rays and the pith and showed an increasing concentration gradient toward the bark. The stem photosynthetic apparatus showed features typical of acclimation to a low-light environment, such as larger grana stacks, lower chlorophyll *a*/*b* and photosystem I/II ratios compared with leaves. Despite likely receiving very few photons, wood chloroplasts were photosynthetically active and fully capable of generating a light-dependent electron transport. Our data provide a comprehensive scenario of the functional features of bark and wood chloroplasts in a woody species and suggest that stem photosynthesis is coherently optimized to the prevailing micro-environmental conditions at the bark and wood level.

Keywords: bark, chlorophyll fluorescence, chloroplast ultrastructure, electron transport, stem photosynthesis, wood.

Introduction

Leaves are the most important photosynthetic organs in most extant vascular plants, but early-diverging tracheophytes also relied on stems to assure a positive carbon gain (Nilsen 1995). Plants void of leaves and with photosynthetically active stems are widely spread in a diversity of ecosystems and families, and comprise both herbaceous and woody species (Gibson 1983, Nilsen 1995, Teskey et al. 2008). These specialized plants are generally found in hot, dry and high-irradiance environments, whereby the more favorable surface-to-volume ratio of stems allows sufficient CO_2 fixation while minimizing water loss to the atmosphere, compared with leaf-level photosynthesis (Gibson 1983, Nilsen 1995). The presence of photosynthetic stems has been documented also in several leaf-bearing species of tropical and temperate habitats, but their possible functional role and contribution to plant metabolism have never been fully elucidated (Nilsen and Sharifi 1994, Pfanz et al. 2002, Ávila et al. 2014).

Functional stomata are frequently observed on the stem surface of herbaceous species, and even of woody plants. These stomatal apertures apparently facilitate carbon uptake from the atmosphere, thus leading to stem-level net photosynthesis, generally indicated as 'stem photosynthesis' (Comstock and Ehleringer 1990, Nilsen 1995, Aschan and Pfanz 2003, Ávila et al. 2014).

Stem photosynthesis comprises both net photosynthesis supplied by atmospheric CO_2 and recycling photosynthesis, which is involved in the re-fixation of internal CO_2 released by respiration from the surrounding heterotrophic stem tissues (Ávila et al. 2014), leading to some carbon recovery with minimal associated water losses. Because the bark limits gas exchange between wood and atmosphere, respiratory CO_2 accumulates

inside the stem reaching concentrations up to 1–26%, thus providing sufficient substrate for photosynthetic activity while also limiting photorespiration (e.g., Cernusak and Marshall 2000, Cernusak et al. 2001, Teskey et al. 2008). Stem photosynthesis may have the additional advantage of maintaining sufficiently high O_2 concentration within the stems, thus preventing the risk of hypoxia (Pfanz et al. 2002, Wittmann and Pfanz 2014). Stem photosynthesis is known to be involved in several processes such as bud development, stem growth, re-sprouting after biotic attack and local exudate synthesis (Saveyn et al. 2010, Cernusak and Hutley 2011, Bloemen et al. 2013*a*, 2013*c*, Steppe et al. 2015). Stem photosynthesis could be also involved in the local supply of energy and photosynthates for embolism repair (Schmitz et al. 2012, Bloemen et al. 2016, De Baerdemaeker et al. 2017, Trifilò et al. 2021). Hence, stem photosynthesis can be a source of sugars that facilitate the generation of osmotic gradients necessary for post-drought refilling of embolized vessels (Zwieniecki and Holbrook 2009, Nardini et al. 2011, Secchi and Zwieniecki 2011, Liu et al. 2019, Secchi et al. 2021).

Stem photosynthetic efficiency depends on chlorophyll content, nitrogen content, structural bark composition and spatial distribution of chloroplasts (e.g., Wittmann et al. 2005, Wittmann and Pfanz 2007, Ávila et al. 2014). Environmental conditions, such as light availability and temperature, also play important roles. Light is necessary for the differentiation of active chloroplasts (van Cleve et al. 1993) so that species-specific differences in axial and radial light transmission through stems might drive the spatial distribution of chloroplasts in different tissues (Schmitz et al. 2012). Depending on bark structural features (e.g., color or thickness), the light reaching the inner portions of stems varies also in quantity and quality. In general, shorter wavelengths are mainly absorbed in the outer bark whereas longer wavelengths penetrate better through the stem (Kharouk et al. 1995, Solhaug et al. 1995, Pfanz and Aschan 2001, Sun et al. 2003).

The amount of light transmitted through stems depends on species and stem age (Wiebe 1975, Aschan and Pfanz 2003, Wittmann and Pfanz 2016). Light transmission and CO_2 fixation usually decrease as stems age and the bark grows thicker (Saveyn et al. 2010). Gradients of light quantity and quality across stems may lead to modifications in relative chlorophyll concentration, chloroplast ultrastructure and photosynthetic efficiency. To date, due to the huge species-specific heterogeneity and the relatively low research efforts on this topic, the information on functional features of stem chloroplasts is still largely fragmented. Recent studies have shown that in some species, the maximum quantum yield of PSII (F_v/F_m) of stem tissues, especially of bark chlorenchyma, has values from 0.71 to 0.81, close to the maximum values recorded for healthy leaves (Damesin 2003, Manetas 2004, Alessio et al. 2005, Manetas and Pfanz 2005, Tausz et al. 2005, Filippou et al. 2007).

Despite this knowledge, it is not clear how the regulation of stem photosynthesis is achieved, and if the photosynthetic efficiency of stem chloroplasts is comparable to that of leaf ones.

Based on the above, refixation of CO_2 by wood photosynthesis might have an important metabolic role (e.g., crucial role in the local production of carbohydrates), while corticular photosynthesis may also fix CO_2 directly transported from the atmosphere through stomata and/or lenticels (Wittmann et al. 2001, Pfanz et al. 2002, Damesin 2003, Alessio et al. 2005, Berveiller et al. 2007, Teskey et al. 2008, Ávila et al. 2014, Vandegehuchte et al. 2015). Thus, according to present knowledge, both bark and wood photosynthesis can contribute to the overall plant carbon economy, but their physiological relevance and the quantitative contribution of stem photosynthesis to the carbon balance of a tree are still unclear (Pfanz 2008, Teskey et al. 2008, Saveyn et al. 2010, Bloemen et al. 2013*b*, 2016).

To gain advanced knowledge on the structure and function of stem chloroplasts, we investigated the ultrastructural, biophysical, biochemical and physiological features of bark and wood chloroplasts in current-year and 1-year-old stems of *Fraxinus ornus* L., a thermophilous, sun-adapted and drought-tolerant deciduous tree (Nardini et al. 2003, 2021, Gortan et al. 2009). We specifically aimed at (i) characterizing light transmission through stems, (ii) identifying radial gradients of chloroplasts distribution and (iii) describing in detail the ultrastructure, functionality and efficiency of stem chloroplasts, compared with chloroplasts found in leaves. We hypothesized that chloroplasts display different characteristics and functionality, depending on the stem region where they are located.

Materials and methods

Plant material

In this study, we have applied to stems several methodologies so far applied only on leaf samples. Therefore, before starting our experimental measurement, we conducted a preliminary analysis to test for the reliability of such methods when used on bark and wood samples. To avoid differences in terms of acclimation to specific growing conditions, all data presented were collected in July 2021 on 3-year-old saplings of *Fraxinus ornus* L. In March 2021, 15 saplings provided by a public nursery (Vivai Pascul, Regional Forestry Service FVG, Tarcento, Italy) were transplanted in 3.5 l pots in a greenhouse at the University of Trieste, Italy (45.66028° N, 13.79550° E). Plants were regularly irrigated at field capacity and their position in the greenhouse was randomly shifted weekly, to assure exposure to uniform light conditions. A slow-release fertilizer (Flortis, universal fertilizer, Orvital, Milano, Italy) was added to each pot in April (4 g) and May (3 g) to prevent nutritional deficiency. Before each measurement (see below), the plants were collected from the greenhouse and moved to the laboratory, and when necessary acclimatized to dark conditions. Analyses were performed on fresh samples of leaves, as well as on stem

samples. Specifically, 1–2 cm long stem segments were cut, and bark and wood were carefully separated both for the current year (B_{cy} and W_{cy}, respectively) and for 1-year-old stems (B_{1y} and W_{1y}, respectively).

For each measure described below, we sampled the stem segments always from the same plant region (i.e., in the apical end of each growth year investigated, about 1 cm below the corresponding apex/node).

Radial light transmission in stems

To characterize light conditions experienced by stem chloroplasts as compared with leaf ones, we initially measured the light transmission spectra through leaves as well as through bark and wood. Measurements were performed when stem cambial cells were active, favoring stem girdling. Accordingly, we separated the bark and wood from a 2-cm-long stem segment to measure the light transmitted from these two stem regions.

The custom-made apparatus used for detecting light transmission in plant samples is illustrated in Figure S1 available as Supplementary data at *Tree Physiology* Online. A light source (KL 2500, Schott, Wolverhampton, UK) providing a photosynthetic photon flux density of 495 μmol m^{-2} s^{-1} was used to illuminate perpendicularly a sample held in place on a wooden stand, at a distance of 20 cm. The stand was covered on the front with a sheet of black plastic to reduce light scattering. A central hole was drilled in the stand and the sample was placed on it to completely cover the hole. A high-resolution fiber-optic connected to a spectrometer (Flame, Ocean Optics) was then placed behind the stand and carefully inserted in the hole of the stand, to measure only the light emitted from the light source and then transmitted through the sample to the fiber. The entire system was placed in a dark room for measurements. Before sample measurements, blank and dark readings were recorded at an integration time (i.t.) of 110 ms. Blank corresponds to the lamp light spectrum measured by spectrometer without any sample, while dark corresponds to the 'dark spectrum', i.e., the spectrum measured with the lamp switched off and with no sample. Measurements were performed on samples obtained from three different saplings, from 400 to 800 nm, at an integration time of 110 ms. All measurements (blank, dark and samples) were repeated 10 times, and the final light transmission spectra were obtained by averaging results. Data were smoothed to eliminate the background instrument error through Origin 9.0 software (Northampton, MA, USA).

Pigment analysis

Since both bark and wood were apparently green (Figure S2 available as Supplementary data at *Tree Physiology* Online), we quantified the pigment contents of these tissues and of leaves upon extraction of fresh material in *N,N′*-dimethylformamide (DMF). Leaves were cut into small pieces to facilitate the extraction, and 50 mg of sample were placed in a 2-ml Eppendorf filled up with 0.5 ml of DMF. The same procedure was applied to bark and wood. For the extraction, 50 mg of bark in 0.5 ml of DMF and 200 mg of wood in 0.75 ml of DMF were used. From each sample, the same amount of fresh material (i.e., 50 mg for leaves and bark, 200 mg for wood) was dried in an oven at 60 °C for 48 h to determine the corresponding dry weight. Samples were kept in the dark at 4 °C for at least 48 h to ensure complete extraction of the pigments and then centrifuged for 3 min at 10,000 r.p.m. Absorption spectra were recorded (Cary 300 UV–Vis, Agilent, USA) between 350 and 750 nm. Pure DMF was used as blank. The final pigment concentration was assessed using Wellburn equations (Wellburn 1994). The pigment analysis was performed on samples obtained from four different saplings.

Epifluorescence and transmission electron microscopy

To investigate chlorophyll distribution along the stem transverse section and to define the chloroplasts structure, fluorescence and electron microscopy analyses were carried out. Light and fluorescent light microscopy analyses were made using a 5000 Leica (Leica, Wetzlar, Germany) microscope, equipped with a digital image acquisition system. A light microscope was used to visualize and describe the various tissues of the stem. Chlorophyll localization was obtained by excitation with UV light. Leaf and stem 40-μm-thick transverse sections were obtained from fresh material with a sliding microtome. Three to five sections per sample were made and analyzed, and observations were repeated for two different saplings, as well as for the following analyses.

For transmission electron microscopy (TEM), fresh samples of leaf, bark and wood were rapidly cut into 2 mm^3 blocks and fixed overnight at 4 °C in 6% glutaraldehyde in 0.1 M sodium cacodylate buffer, with a pH 6.9, and then fixed for 2 h in 1% osmium tetroxide in the same buffer. The samples were dehydrated in a graded series of ethanol and propylene oxide and finally embedded in Araldite. Ultrathin sections (80–100 nm) were prepared with an ultramicrotome (Ultracut; Reichert-Jung, Vienna, Austria) and treated with lead citrate and uranyl acetate. Samples were analyzed with a transmission electron microscope (Tecnai G2; FEI, Hillsboro, OR, USA) operating at 100 kV. We analyzed images (n = 8–15 images per each tissue) with ImageJ to obtain data on grana number, starch number and stromal area, following Mazur et al. (2021). Due to the hardness of the material, the image quality of wood samples did not allow us to make accurate measurements of the number of stromal thylakoids, and we can only draw some conclusions from a visual/descriptive analysis of the images.

Fluorescence spectroscopy

To quantify the relative fluorescence intensities emitted from PSI (F735 nm) and PSII (F685 and F695 nm), we

characterized the low-temperature (77 K) chlorophyll fluorescence emission spectra of leaves, bark and wood. The 685- and 695-nm fluorescence emission components originate from the antenna complex and reaction center of PSII subunits CP43 and CP47, respectively (Krause and Weis 1991, Govindjee 1995, Andrizhiyevskaya et al. 2005, Lamb et al. 2015). The fluorescence emission band at 735 nm is instead due to PSI and its associated light-harvesting complex I (LHCI; Breton 1982, Krause and Weis 1991, Govindjee 1995, Morosinotto et al. 2003, Dobrev et al. 2016, Dymova et al. 2018, Lamb et al. 2018). Therefore, these LT fluorescence spectra give information on the relative composition of photosynthetic apparatus. Specifically, the F735/695 ratio provides a reliable estimate of the distribution of excitation energy to each of the photosystems and/or their relative abundance within the thylakoid membranes (Krause and Weis 1984).

Fresh material (i.e., 50 mg for leaves and bark, 200 mg for wood) was rapidly cut into small pieces and finely ground with liquid nitrogen in a mortar. The material was then quickly transferred in a 2-ml Eppendorf with 0.5 ml of 60% w/v glycerol, 10 mM Hepes, pH 7.5. Each sample was set up for the measurements in a glass Pasteur pipette and put in a Dewar vessel filled with liquid nitrogen. Low-temperature (77 K) emission spectra measurements were performed through a fluorimeter (Varian Cary Eclipse, Agilent, USA), exciting samples at 440 nm (excitation and emission slits were set to 2.5 nm) and recording the emission spectra from 600 to 800 nm. Data for W_{1y} were smoothed to eliminate the background instrument error through Origin 9.0 software (Northampton, MA, USA).

SDS-PAGE electrophoresis and western blot analysis

Western blot analyses were performed to evaluate the composition of the photosynthetic apparatus of bark and wood compared with the leaves. Total protein extracts were obtained from fresh material (i.e., 50 mg for leaves, 110–130 mg for bark, 200–300 mg for wood) finely ground with liquid nitrogen in a mortar. The material was then quickly put in a 2-ml Eppendorf with 0.5 ml of sample buffer (SB) 3× (125 mM TRIS pH 6.8, 100 mM DTT, 9% (w/v) SDS and 30% (w/v) glycerol) for leaves and bark and 700 μl SB3× for wood. The protein concentration of extracts was quantified using the BCA protein assay, and samples were loaded accordingly to the quantification (1× samples corresponding to 10 mg μl^{-1}) in an acrylamide gel at a final concentration of 12%. Western blot analysis was performed by transferring the protein to nitrocellulose (Bio Trace, Pall Corporation, Auckland, New Zealand). The membranes were hybridized with specific primary antibodies: anti-PsaA (Agrisera, catalogue number AS06172), custom-made anti-D2, anti-PsbS (Storti et al. 2020); custom-made anti-RuBisCo, anti-LHCII and anti-CP47 were also used. After hybridization, signals were detected with an alkaline phosphatase-conjugated antibody (Sigma Aldrich, Italy). Measurements were repeated for three different saplings.

In vivo imaging fluorescence measurements

Photosynthetic efficiency of leaves, bark and wood was estimated by *in vivo* chlorophyll fluorescence measurements, using a closed-imaging PAM chlorophyll fluorometer (Photon Systems Instruments, Brno, Czech Republic).

Saplings were dark-acclimated for at least 1 h before measurements. Leaf and stem segments ∼1-cm long were sampled from four different saplings. Bark and wood were separated, and wood segments were sectioned both longitudinally and radially. Samples were placed in a Petri dish resting on damp paper and were maintained hydrated by covering them with a thin layer of distilled water. The petri dish was then placed in the closed-imaging PAM chlorophyll FluorCam to obtain chlorophyll fluorescence images.

The optimal quantum yield of PSII (F_v/F_m) was measured for the different areas of internal stem tissues (Maxwell and Johnson 2000).

Spectroscopy measurements

In vivo spectroscopic analysis was performed to gain insights into the regulation of electron flow via absorbance changes. The measurements were performed at room temperature with a JTS-10 spectrophotometer (Bio-Logic, France) on fresh samples of leaf, bark and wood collected from the same sapling and repeated for five different saplings. The plants were dark-acclimated for 1 h before measurements. We separated bark and wood from a 1-cm-long stem segment. For the wood, we prepared longitudinal thin sections to place on the sample holder. The samples were kept hydrated by wrapping them in a transparent cellulose filter.

An alternative and more precise method to assess photosynthetic activity is to monitor the electrochemical gradient across thylakoid membranes as generated during photosynthesis, using the electrochromic shift (ECS; Witt 1979, Bailleul et al. 2010, Allorent et al. 2015, 2018). Such a signal is in fact modified when light drives an electron transport and thus the generation of an electrochemical gradient. An evaluation of functional photosynthetic complexes and electron transport rates (ETRs) was done by measuring the ECS, according to the protocol described by Bailleul et al. (2010) and Mellon et al. (2021). The ECS signal provides accurate data on the function of the photosynthetic complexes (Bailleul et al. 2010), and photosystem charge separation can be evaluated by DIRK (dark-induced relaxation kinetic, Sacksteder and Kramer 2000). The ETR was obtained by subtracting the slope of ECS during the dark (SD) from the slope in the light (SL) and normalized to the total PSs content (PSI + PSII). To remove the contribution of scattering and cytochromes, the background signal at 546 nm was subtracted from the 520-nm signal. Functional total photosystems (PSs)

were quantified using a single flash turnover emitted by a xenon lamp (Gerotto et al. 2016).

P700 concentration was measured at 705 nm using an extinction calculated from Ke (1972). Samples were illuminated with continuous red (630 nm) light, which was transiently switched off to measure P700 absorption changes at 705 nm. Each measurement was repeated on three to eight different saplings.

Statistics

All statistical analyses were performed with R software (R Core Team 2021). The normality of residuals and homogeneity of variances were tested, and when these assumptions were not violated, one-way ANOVA analysis through 'aov' function in 'stats' R package was used. For significance tests, post-hoc Tukey's Honestly Significant Difference test (Tukey HSD) was performed through 'Tukey HSD' function in 'stats' R package.

When the homogeneity of variances assumption was violated, generalized least square (GLS) models were performed, using 'gls' function including the 'varPower' variance structure. Pigments data were log-transformed to respect the assumption of normality, before performing GLS model. Differences between groups were tested post hoc with 'Holm' contrasts using the *emmeans* function (*emmeans* package).

Results

Light transmission in stems

Measurements of light transmission through the bark (B_{cy} and B_{1y}) and wood (W_{cy} and W_{1y}) of different ages and through leaves revealed a progressive modification of light quantity and quality (Figure 1 and Figure S3 available as Supplementary data at *Tree Physiology* Online). The transmission spectra of B_{cy} and B_{1y} were very similar to that of the leaf. All these spectra showed a peak at 550 nm and suggested a maximum light absorption between 400–500 and 600–700 nm, as expected from chlorophyll-containing samples. W_{cy} and W_{1y} also showed decreases in transmission at 400–500 and 600–700 nm associated with chlorophyll absorption. They also showed a significant contribution at all wavelengths associated with scattering. The analysis of non-normalized spectra (Figure S3 available as Supplementary data at *Tree Physiology* Online) clearly shows that while light can penetrate both bark and wood, its transmission is attenuated going from leaves to bark to wood. Photons were better transmitted through the xylem to the pith in the younger stem, compared with the 1-year-old one. Moreover, blue and red light was highly absorbed in the bark, while green- and far-red light penetrated much better toward the xylem parenchyma. The observed transmission spectra suggested a change in light quantity and quality from the outermost toward the innermost portions of the stem. This indicated that the inner stem compartments are reached by limited light intensity, also with an altered spectrum.

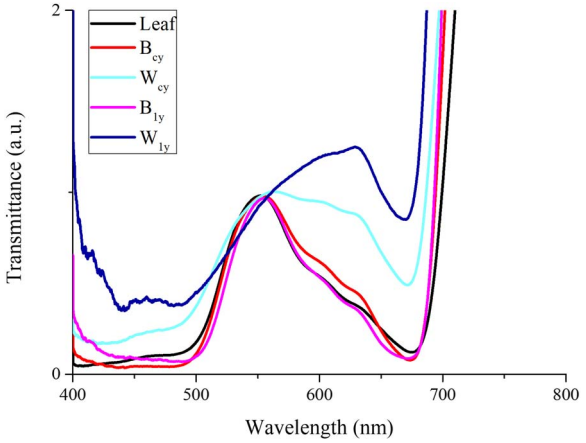

Figure 1. Light transmission spectra of leaf, bark and wood of current (B_{cy} and W_{cy}) and 1-year-old stems (B_{1y} and W_{1y}) of *Fraxinus ornus* L. Data normalized at 550 nm (arbitrary units). Each measurement was replicated 10 times and the average value was calculated. Spectra were corrected for dark pixels.

Bark and wood chloroplasts of F. ornus saplings acclimate to light conditions

Chlorophylls and carotenoids were detected throughout the stem, both in the bark and in the wood. In both compartments, chlorophyll (Chl) content was lower compared with leaves. However, the Chl content of bark was higher than that of wood (Table 1). The pigment concentration in the bark decreased with increasing stem age. This was also coupled to a qualitative change, with a relatively larger decrease of chlorophyll *a* (Chl*a*) as compared with chlorophyll *b* (Chl*b*) (Table 1). Therefore, the Chl*a*/*b* ratio of the leaf was similar to that of B_{cy}, while it decreased progressively in B_{1y}, W_{cy} and W_{1y} (Figure 2A). Chl*a*/*b* of W_{cy} and W_{1y} was significantly lower compared with leaf, B_{cy} and B_{1y} ($P < 0.0005$ and $P < 0.05$, respectively, Figure 2A).

Carotenoid (Car)/Chl ratios were similar in leaves, B_{cy} and B_{1y}, with a slight relative increase in W_{1y} and W_{cy} (Figure 2B).

The Chl distribution and ultrastructural features of chloroplasts were further investigated for leaves, B_{cy}, W_{cy}, B_{1y} and W_{1y}, by epifluorescence and TEM. A detailed anatomical transverse section is presented in Figure S4 available as Supplementary data at *Tree Physiology* Online, showing the different tissues composing the bark, i.e., periderm, cortex and phloem (Angyalossy et al. 2016).

Analyses showed that the majority of stem Chl was present in the bark mainly in the parenchyma cells of phelloderm, cortex and phloem, but chlorophyllous cells were detected also along xylem rays and around the pith (Figure 3). At higher

Table 1. Chlorophyll *a* (Chl*a*), chlorophyll *b* (Chl*b*), total Chl (Chl*a* + Chl*b*) and carotenoid (Car) concentration for leaf, bark and wood of current (B_{cy} and W_{cy}) and 1-year-old stems (B_{1y} and W_{1y}) of *Fraxinus ornus* L. Mean values are reported ± SD ($n = 4$). Different letters indicate significant differences between samples ($P < 0.05$).

Sample	Chl*a* (mg g^{-1} FW)	Chl*b* (mg g^{-1} FW)	Total Chl (mg g^{-1} FW)	Car (mg g^{-1} FW)
Leaf	2.589 ± 0.801 a	0.949 ± 0.336 a	3.538 ± 1.136 a	0.514 ± 0.139 a
B_{cy}	0.409 ± 0.136 b	0.165 ± 0.061 b	0.574 ± 0.196 b	0.076 ± 0.024 b
B_{1y}	0.293 ± 0.076 b	0.126 ± 0.040 b	0.419 ± 0.117 b	0.060 ± 0.015 b
W_{cy}	0.018 ± 0.009 c	0.008 ± 0.004 c	0.026 ± 0.012 c	0.004 ± 0.001 c
W_{1y}	0.018 ± 0.005 c	0.009 ± 0.002 c	0.027 ± 0.007 c	0.005 ± 0.001 c

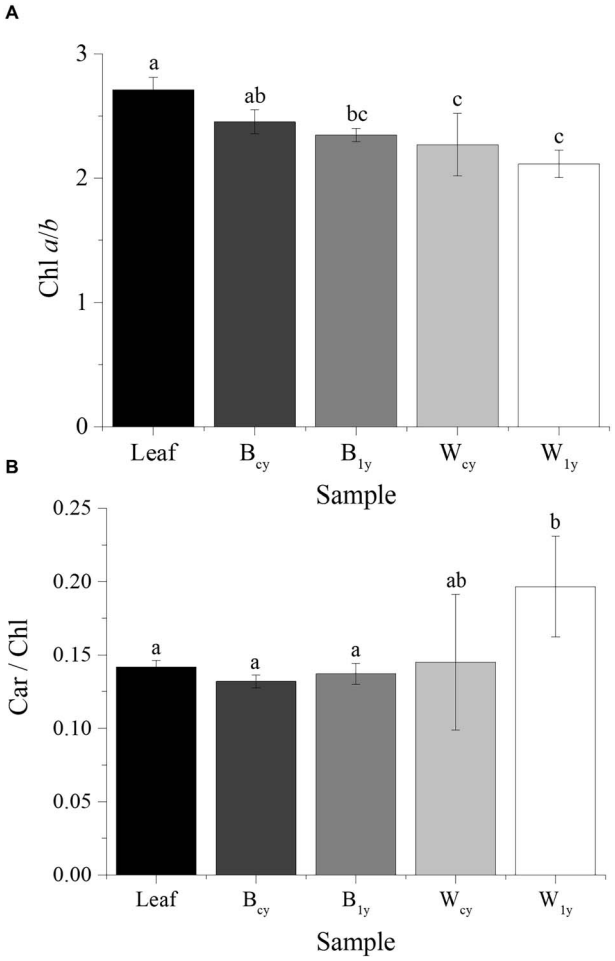

Figure 2. Mean chlorophyll *a*/*b* (Chl*a*/*b*) (A), carotenoids/total chlorophyll (Car/Chl) (B) comparison between leaf, bark and wood of current (B_{cy} and W_{cy}) and 1-year-old stems (B_{1y} and W_{1y}) of *Fraxinus ornus* L. Standard deviation bars are included on each of the bar graphs ($n = 4$). Different letters indicate significant differences between samples ($P < 0.05$).

magnification, plastids are visible as chlorophyll autofluorescence in red, whereas the green color is given by lignified or suberified components. Electron microscopy analysis defined the ultrastructure of stem chloroplasts that showed intact and well-defined organization (Figure 4 and Figure S5 available as Supplementary data at *Tree Physiology* Online). Figure S5 available as Supplementary data at *Tree Physiology* Online, reports images acquired at lower magnification, useful to visualize the general features of the different tissues. Figure 4 shows images at higher magnification to better appreciate the different characteristics of the chloroplast ultrastructure and thylakoid distribution.

The phelloderm cells contained well-developed chloroplasts, with both stroma lamellae and grana stacks resembling those of leaves (Figure 4B and D, Table S1 available as Supplementary data at *Tree Physiology* Online). Chloroplasts found in the phloem presented a significantly lower number of grana (Table S1 available as Supplementary data at *Tree Physiology* Online), with more stacks (Figure S5 available as Supplementary data at *Tree Physiology* Online). A significant reduction of the stromal area was observed from bark to wood, specifically between chloroplasts found in the phelloderm/cortex and those in the wood of both growth years (Table S1 available as Supplementary data at *Tree Physiology* Online). A similar starch amount was found in the chloroplasts of different samples.

Finally, chloroplasts found in the wood of each growth year apparently have very few stromal thylakoids (Figures S4 and S5E and F available as Supplementary data at *Tree Physiology* Online).

Changes of composition of photosynthetic apparatus in different tissues

Upon excitation at 440 nm, the low-temperature (LT, 77 K) fluorescence emission spectra of leaves, bark and wood of current and 1-year-old stems showed three major emission bands (685, 695 and 735 nm) (Figure 5A).

As shown in Figure 5A, there is a significant decrease in the relative intensity of fluorescence from the PSI and LHCI complexes (at 735 nm) in B_{cy} and B_{1y}. This trend is further amplified in W_{cy} and W_{1y}. In accordance, the F735/F685 ratio (Figure 5B) gradually decreased from bark to wood. Such a lower value of the ratio for bark and wood compared with leaf suggests a reduced content of PSI complexes relative to PSII.

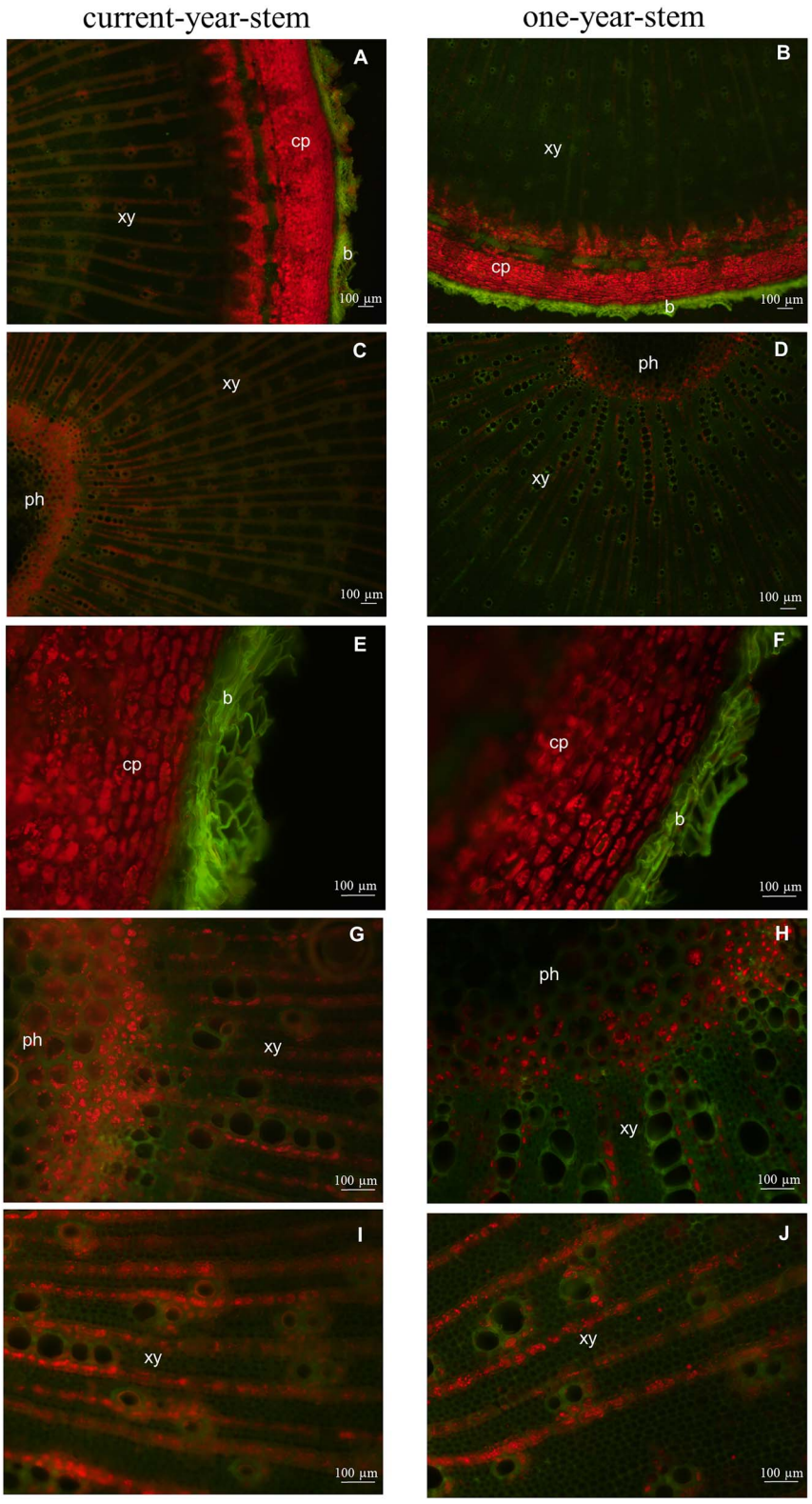

Figure 3. Representative transverse-section images of current year and 1-year-old stems of *Fraxinus ornus* L. observed by epifluorescence microscopy. The red color is given by chlorophyll fluorescence when excited by UV light; the green color is given by lignified or suberified components. Periderm of current (A, E) and 1-year-old stems (B, F). Xylem rays and pith of current (C, G, I) and 1-year-old stems (D, H, J). Abbreviations: b, phellem; cp, cortical parenchyma; xy, xylem; and ph, pith.

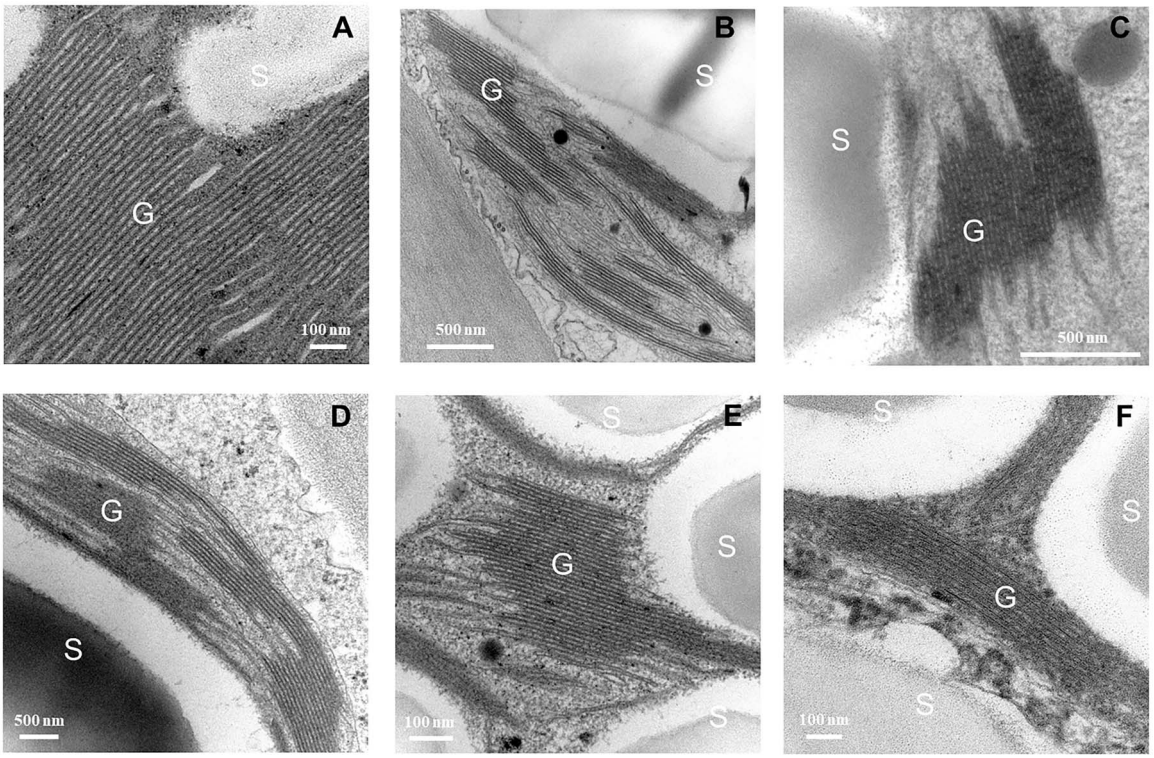

Figure 4. Representative electron micrographs of chloroplast thylakoids of different stem samples of *Fraxinus ornus* L. (A) Leaf; (B) periderm of current year stems; (C) xylem rays of wood of current year stems; (D) cortical parenchyma of 1-year-old stems; (E) phloem of 1-year-old stems; (F) xylem rays of 1-year-old stems. Abbreviations: G, grana thylakoids; S, starch.

The F685/F695 ratio (Figure 5C) of B_{cy} and B_{1y} was similar to that of both leaf and wood. Compared with the leaves, the values were significantly higher for both W_{cy} and W_{1y}. The alteration in the F685/F695 ratio might be attributed to a relative increase in the fluorescence emitted by the antenna system of PSII with respect to the reaction center.

Photosynthetic apparatus composition was also investigated using specific antibodies. An equal protein amount was loaded for each sample (Figure 6). As expected, samples that accumulated less Chl also showed a lower abundance of photosynthetic proteins. Nevertheless, western blot analysis allowed the detection of LHCII protein in all samples investigated, confirming their presence even in wood.

RuBisCO was also detected in all samples, i.e., leaf, bark and wood, with a signal progressively lower and particularly weak in the latter. Photosystem I reaction center subunit II, chloroplastic (PSAD) was detected in leaf and B_{cy}, whereas only a faint band was detected in B_{1y}. No PSAD signal was detected for the wood. The band of D2 proteins was detected only in the leaf and weakly in B_{cy}.

The stem contains photosynthetically active cells

Chlorophyll fluorescence imaging (Figure 7A) across longitudinal sections of current- and 1-year-old stems detected significant signals, consistent with all the above results. Analysis of maximal PSII photochemical efficiency (F_v/F_m) showed that leaf, B_{cy}, W_{cy}, B_{1y} and W_{1y} have no statistically significant different activities (Figure 7B). This means that even in wood, PSII displays a maximum potential quantum efficiency resembling the one of leaves.

Despite the non-ideal optical features of the samples and the presence of a strong scattering, we were able to detect for the first time an ECS signal also in bark and wood samples (Figure S6 available as Supplementary data at *Tree Physiology* Online). These results demonstrate the presence of an active photosynthetic electron transport in illuminated tissues mediated by PSI and PSII charge separation activity capable of generating and sustaining a membrane potential, clearly confirming that the photosynthetic apparatus of both bark and wood is fully functional.

The ETR was quantified by comparing the ECS when the light was switched off (S_D) and when the light was on (S_L) (Figure 8A), an approach that enables to distinguish the light-dependent signal from other contributions. Even if the ETR values should be considered semi-quantitative because of the inability to use inhibitors in these samples for internal standardization (see Materials and methods for details), data indicate that B_{cy} ETR was comparable to that of the leaf, while a lower electron transport capacity was observed with

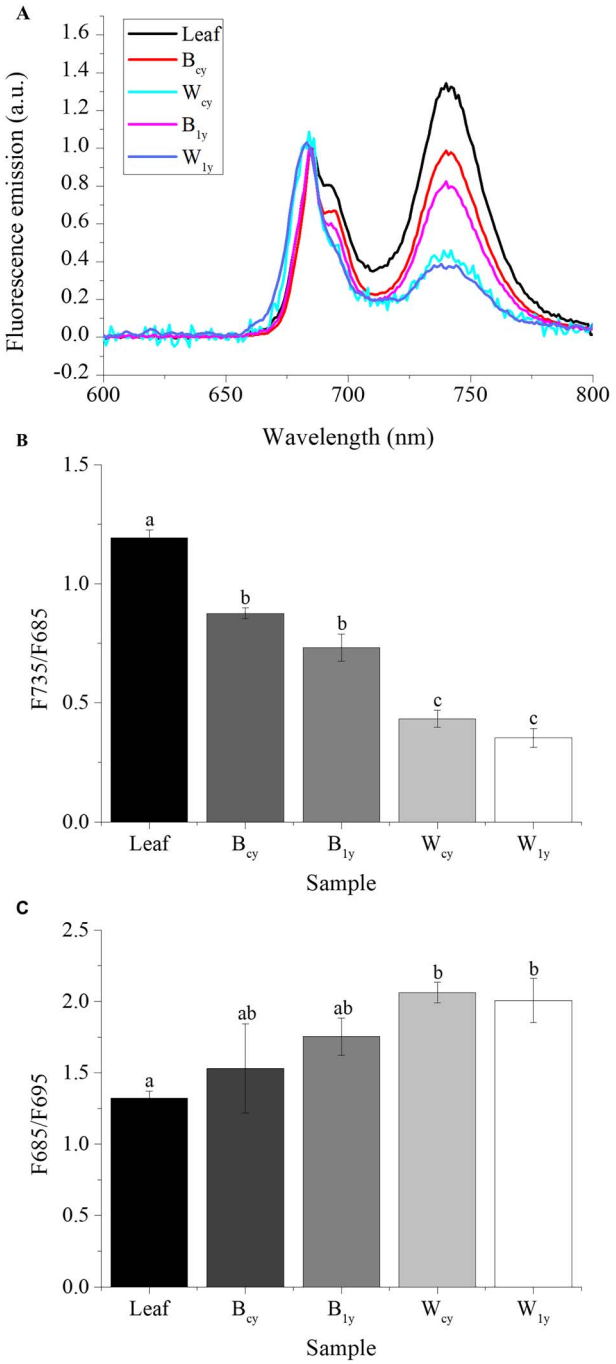

Figure 5. (A) 77-K fluorescence emission spectra of leaf, bark and wood of current (B_{cy} and W_{cy}) and 1-year-old stems (B_{1y} and W_{1y}) stems of *Fraxinus ornus* L. Spectra are normalized on PSII emission (685 nm). Excitation wavelength was 440 nm. (B) Fluorescence ratio F735/F685 and (C) F685/F695 for leaf, bark and wood of current (B_{cy} and W_{cy}) and 1-year-old stems (B_{1y} and W_{1y}). Mean values are reported ± SD ($n = 2$). Different letters indicate significant differences between samples ($P < 0.05$).

increasing stem age in B_{1y} (Figure 8B). ETR in the wood (both W_{cy} and W_{1y}) was even lower compared with leaf and B_{cy}.

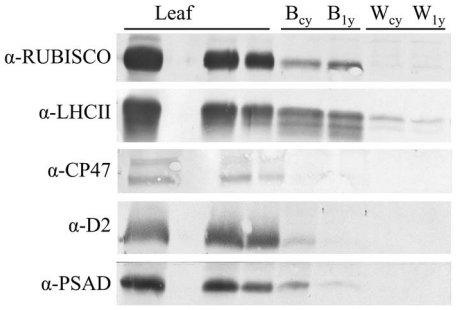

Figure 6. Immunoblot analysis of leaf, bark and wood of current year (B_{cy} and W_{cy}) and 1-year-old stems (B_{1y} and W_{1y}) of *Fraxinus ornus* L., using antibodies against different components of the photosynthetic apparatus from RuBisCo, antenna complexes (LHCII, CP47), PSII (D2) and PSI (PSAD). Different dilutions of total protein extracts were loaded. The first column of leaf, B_{cy}, B_{1y}, W_{cy} and W_{1y} were loaded with 1×, which corresponds to 10 mg μl^{-1} of total proteins. The second and third columns of leaf have 0.2× and 0.5× (RuBisCo, LHCII), 0.25× and 0.13× (CP47), and 0.33× and 0.16× (D2, PSAD), respectively.

A further confirmation that photosynthesis is fully functional in these tissues can be obtained by looking at the oxidized P700 ($P700^+$) signal (Figure 9A). When P700 is oxidized during photosynthesis, it generates a difference in absorption at 705 nm that can be detected. Since this signal only detects a difference in absorption generated by light, it demonstrates the presence of a photo-oxidizable PSI, enabling to distinguish it from other optical signals. As shown in Figure 9A, all samples show the ability to generate a $P700^+$ signal dependent on illumination. The signal is high in samples such as leaves and bark, where Chl (and PSI) content is higher.

Figure 9B shows in more detail the reduction kinetics of P700 when the light is switched off after illumination with actinic light. When the light is switched off, the $P700^+$ is reduced back to P700 restoring the initial level of light absorption. Since samples are pre-illuminated for several minutes and have fully activated steady photosynthetic activity, the kinetics of P700 reduction are indicative of their electron transport capacity. These measurements show a much faster re-oxidation in leaf samples, indicative of a higher electron transport capacity. On the other hand, the kinetic is much slower for B_{cy} (τ: 66.45 ± 1.06 ms), W_{cy} (τ: 57.15 ± 18.19 ms), B_{1y} (τ: 50.18 ± 22.37 ms) and W_{1y} (τ: 37.13 ± 22.92 ms) compared with leaves (τ: 17.69 ± 9.87 ms), indicating a lower electron transport activity in these samples.

Discussion

Our study represents one of the first examples of an in-depth analysis of ultrastructural and functional features of bark and wood chloroplasts and stem photosynthetic activity. Our data offer new insights into the functional traits of the photosynthetic apparatus in the different stem regions.

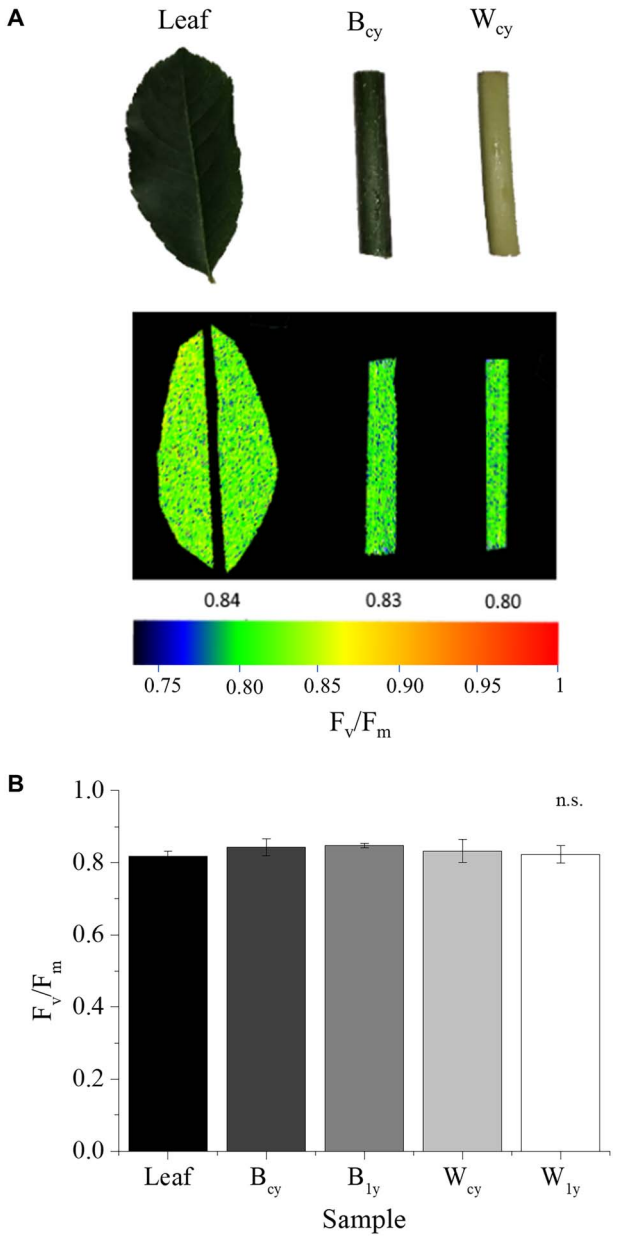

Figure 7. (A) Example of optical analysis of leaf, bark and wood of current year stem (B_{cy} and W_{cy}) of *Fraxinus ornus* L. to analyze the different photosynthetic efficiency, shown in terms of maximum quantum efficiency (F_v/F_m) of PSII. (B) Maximum quantum efficiency (F_v/F_m) of PSII of leaf, bark and wood of current year (B_{cy} and W_{cy}) and 1-year-old stems (B_{1y} and W_{1y}) of *Fraxinus ornus* L. Mean values are reported ± S.D. ($n = 4$); n.s.: not statistically significant.

Light environment across the stem section

Transmission of light through isolated portions of bark and wood of *F. ornus* changed with stem age, decreasing from current-year to 1-year-old stems. This can be explained by the gradual increment of the protective cork tissues (Pilarski 1989, Aschan et al. 2001, Pfanz and Aschan 2001, Filippou et al. 2007). The optical properties of stems resulted in a different light environment between bark and wood compartments in terms of both intensity and spectral composition. The blue band of the spectrum is mainly absorbed by the bark, and consequently, the wood is reached by green- and far-red-enriched light. Our findings strongly suggest that light is attenuated when traveling through the wood layer and are in accordance with previous studies (e.g., Pfanz and Aschan 2001, Pfanz et al. 2002, Manetas and Pfanz 2005, Wittmann and Pfanz 2016), which also showed that stems absorb most of the visible spectrum, except for far-red light that might be conducted also in the axial direction of stems and roots (Sun et al. 2003, 2005).

Pigment composition and chloroplasts' structure

Despite the low light transmittance in the radial stem direction, we could confirm the presence of Chl and Car in both bark and wood of *F. ornus* stems. This was evident in fluorescence microscopy images, showing Chl accumulated in the bark (in the parenchyma cells of phelloderm, cortex and phloem) but also present along the xylem rays and around the pith. The detailed analysis, however, revealed a gradual decrease in the concentration of both pigments going from leaves to bark and wood, and also with the tissue age (Table 1). For this reason, we deemed it important to compare the chloroplast ultrastructure and photosynthetic apparatus organization and function of stems and leaves. In accordance with previous observations (Larcher et al. 1988, Ivanov et al. 1990, Pfanz et al. 2002, Liu et al. 2021), leaf and stem chloroplasts had different ultrastructural organization. In particular, within the stem radial profile, from the outer to the inner tissues, there is a clear pattern with progressively larger grana, smaller stroma lamellae and lower stromal area in the wood (mostly occupied by accumulated starch). These modifications in the chloroplasts' ultrastructure along the stem profile are likely induced by the gradient in light quantity/quality. As previously suggested by other researchers (e.g., Larcher et al. 1988, Ivanov et al. 1990, Pfanz et al. 2002, Hu et al. 2021, Liu et al. 2021), broader grana stacks are fundamental to harvest the limited light energy penetrating through the stem, and highly stacked thylakoid membranes are a typical acclimation response to low light environments.

Light is an important requisite for the differentiation of active chloroplasts, but Chl can be synthesized at light intensities below those necessary to fuel the photosynthetic process, suggesting that the mere presence of pigments does not necessarily indicate active photosynthesis in stem chloroplasts (Schaedle 1975). Consistently with the observed light gradient (e.g., Larcher et al. 1988, van Cleve et al. 1993, Pilarski 1999, Pfanz et al. 2002, Filippou et al. 2007, Wittmann and Pfanz 2016), a progressive decrease of Chl*a*/*b* ratio was also observed in *F. ornus* when moving into innermost stem regions (Figure 2), suggesting that chloroplasts are acclimated to lower light availability. The analysis of wood samples is particularly interesting since they show other typical features of acclimation to a low light environment, such as a lower Chl*a*/*b* ratio, larger

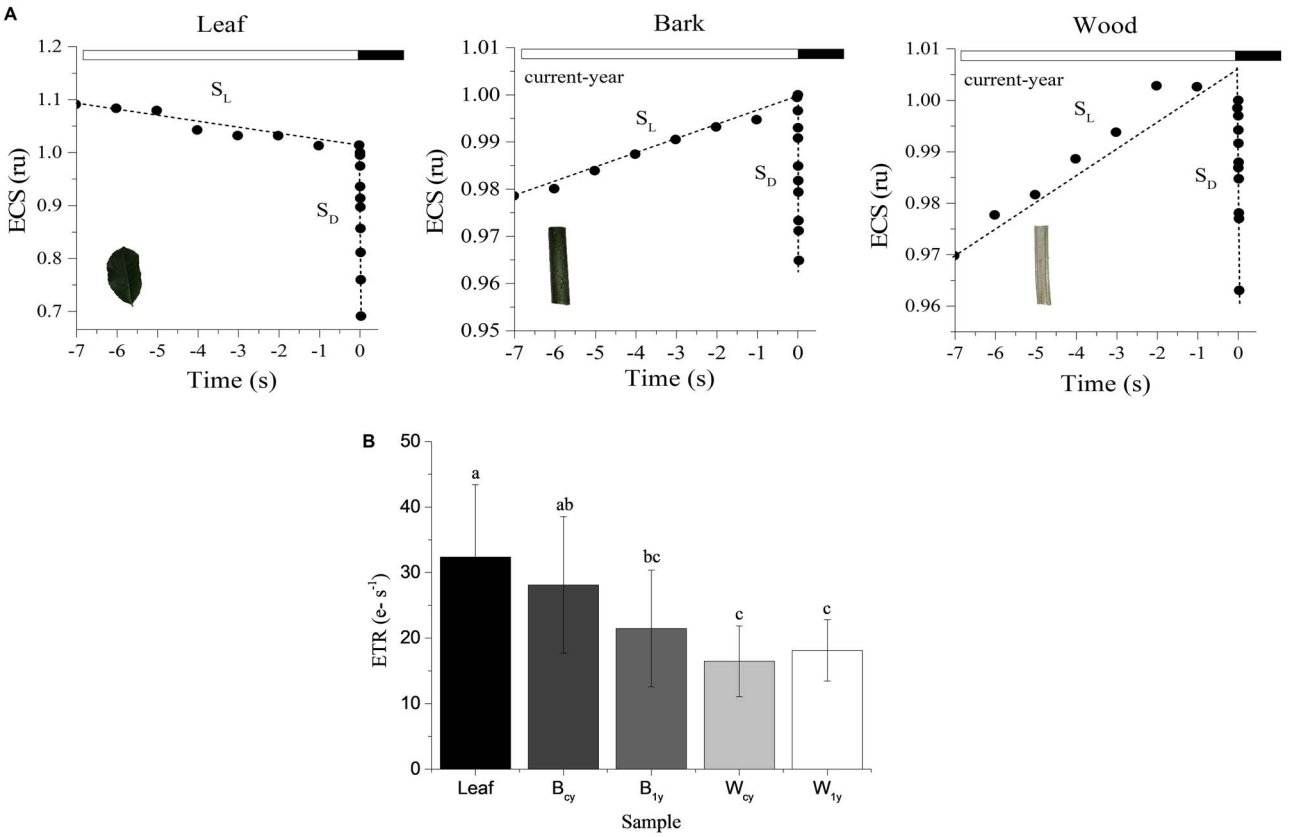

Figure 8. (A) Examples of changes in the ECS signal measured at 520–546 nm upon normalization on the first data point in the dark to one, to allow for a better comparison. A slope of the ECS changing during a transition from light (S_L) to dark (S_D) is reported for leaf, bark and wood of current year (B_{cy} and W_{cy}) of *Fraxinus ornus* L. White box: the actinic light was on; black box: the actinic light was switched off. (B) ETR of leaf, bark and wood of current year (B_{cy} and W_{cy}) and 1-year-old stems (B_{1y} and W_{1y}) of *Fraxinus ornus* L. Data are normalized on functional total photosystems (PSs). The error bars represent mean values ± SD ($n \geq 5$). Different letters indicate significant differences between samples ($P < 0.05$).

number of grana stacks and higher PSII/PSI ratios (Anderson et al. 1973, Lee and Whitmarsh 1989, Brugnoli et al. 1994, Murchie and Horton 1997). All these findings suggest efficient optimization of the stem photosynthetic apparatus to low and red-enhanced irradiation, especially in the wood parenchyma.

Any change in light quantity/quality can induce modifications in the structure and organization of the main pigment-protein complexes of chloroplasts (Anderson et al. 1995, 2012, Eberhard et al. 2008, La Rocca et al. 2015, Albanese et al. 2016, Storti et al. 2020). Indeed, PSI is preferably excited by far-red light ($\lambda > 700$ nm), whereas PSII absorbs better at wavelengths shorter than 680 nm (Chow et al. 1990). An increase in red and far-red light is expected to induce an increase of the PSII abundance and a decrease in that of PSI and, hence, a decrease in PSI/PSII ratio in order to maintain an equal electron transport capacity of the two photosystems despite the different excitation levels (Ruban and Johnson 2009, Lemeille and Rochaix 2010, Minagawa 2011, Mukherjee 2020, Hu et al. 2021). In line with this, the low temperature (77 K) peak of the PSI-related complex was much lower in bark and wood than in leaves of *F. ornus*, indicating lower relative accumulation of PSI proteins, consistent with previous studies (Ivanov et al. 1990, 2006). This also supports the hypothesis that wood chloroplasts are acclimated not only to low light but also to a different light spectrum, enriched in far-red wavelengths. Overall, data suggest the ability of stem chloroplast to modify the stoichiometry of the two photosystems to retain a high quantum efficiency of photosynthesis as observed in plants exposed to different light regimes (Chow et al. 1990), and thus an acclimation response, dynamically modifying the composition and function of thylakoids membranes in response to different light conditions, is activated here (Melis and Harvey 1981, Anderson 1986).

Chloroplasts activity/efficiency

In addition to their capability of activating an acclimation response, bark and wood chloroplasts had PSII with good photochemical activity, as shown by F_v/F_m values similar to those measured for leaves (Björkman and Demmig 1987). Our results are in line with other studies focused on current-year stems of several deciduous species (Damesin 2003, Manetas and Pfanz 2005, Berveiller et al. 2007, Wittmann and Pfanz 2007, 2008). The novel data that we present in this paper have been acquired using ECS spectroscopy applied to the analysis

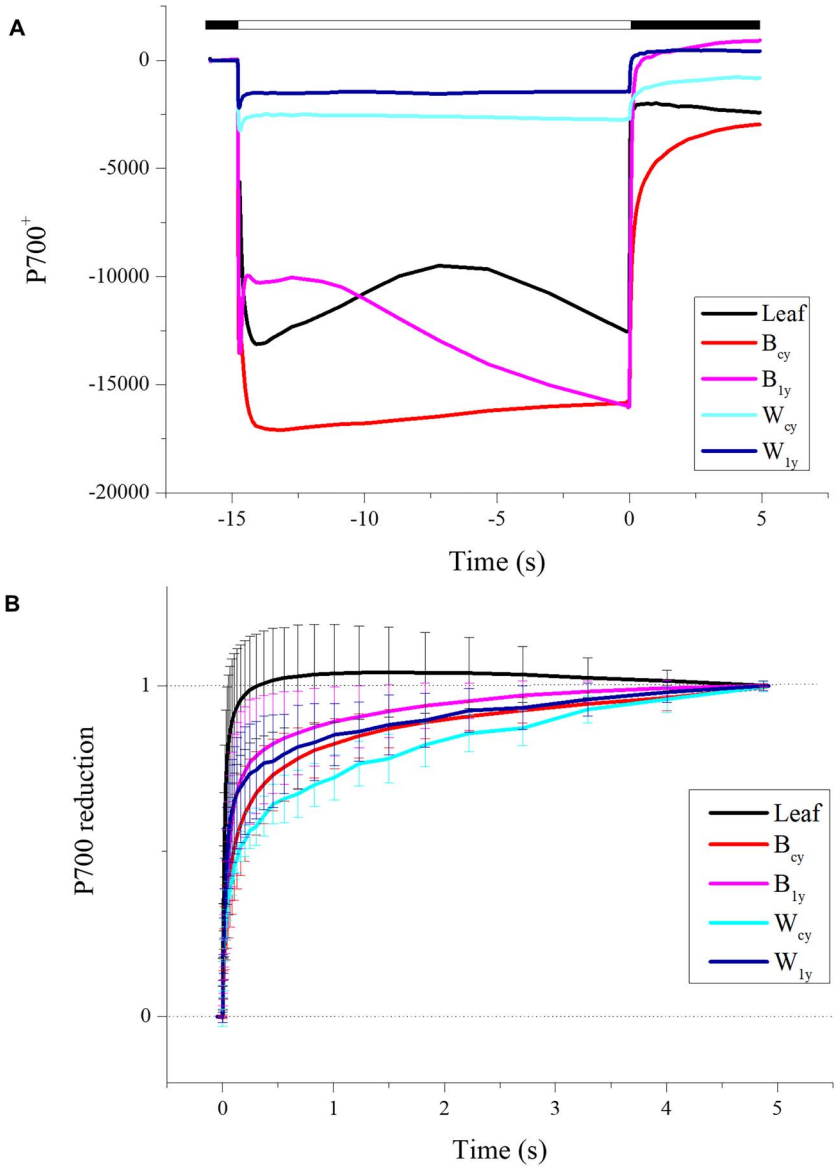

Figure 9. (A) Examples of oxidation of P700 ($P700^+$) kinetics of leaf, bark and wood of current year (B_{cy} and W_{cy}) and 1-year-old stems (B_{1y} and W_{1y}) of *Fraxinus ornus* L. White box: the actinic light was on; black box: the actinic light was switched off. (B) $P700^+$ reduction kinetics of leaf, bark and wood of current year (B_{cy} and W_{cy}) and 1-year-old stems (B_{1y} and W_{1y}) of *Fraxinus ornus* L. curves shown are average of three to eight independent measurements.

of bark and wood chloroplasts. With this methodology, we were able to quantify the number of active PSs for each sample type, thus determining the effective ETR for leaves, bark and wood. Using ECS spectroscopy, it was also possible to demonstrate that bark and wood chloroplasts are capable of light-dependent electron transport. Moreover, the bark of current-year stems had similar photosynthetic capacity, measured by ETR, as leaves. In older stems, the bark ETR decreased, whereas the photosynthetic capacity of wood was lower compared with both bark and leaves. Interestingly, all these results suggest that current-year bark has photosynthetic characteristics comparable to those of the leaves, as already noted by Berveiller et al. (2007). Data on the photochemical activities of PSII and PSI show that the few chlorophyllous cells buried deep in the wood are still able to perform photosynthesis. Indeed, as expected, the size of $P700^+$ re-reduction was lower in bark and wood than in leaves, suggesting a lower potential electron transport activity, which is also in agreement with the lower abundance of PSI found with immunoblot analysis (Figure 6). Finally, this hypothesis is supported also by the presence of LHCII proteins in the bark as well as in wood that suggested efficient light-harvesting for the photosystems in stems even in the low-light environment. Indeed, LHCII is an antenna that can connect energetically the entire photosynthetic apparatus,

both PSI and PSII, and according to different light intensities can associate preferentially to one PS rather than the other (Wientjes et al. 2013, Grieco et al. 2015).

To summarize, stem chloroplasts accumulate relatively more LHCII and PSII, by increasing the amount of thylakoid membrane stacking. On the other hand, they show less PSI and fewer stroma lamellae than leaves. Once again, these characteristics are a typical acclimation response to a red-enhanced and low-light environment, to increase light use efficiency. Many of these characteristics have been observed also in shade leaves. Compared with sun leaves, shade leaves show more grana stacks, lower Chl*a*/*b* ratio and higher numbers of light-harvesting complexes per reaction center (e.g., Lichtenthaler et al. 1981, 2013, Anderson 1986, Ballottari et al. 2007, Flannery et al. 2021).

Our data thus provide support for the hypothesis that chlorophyll-containing cells near the vascular system, in a region receiving mostly green or far-red light, are indeed photosynthetically active. On the other hand, the precise physiological role of this photosynthetic activity still needs to be explored and proven (Pfanz and Aschan 2001, Hibberd and Quick 2002, Berveiller and Damesin 2008).

Available data on the enzymatic features of bark and wood photosynthesis are particularly scarce in the literature. The presence of RuBisCo was detected in leaves and bark and weakly in the wood, indicating a capacity to fix CO_2 also in the stem compartments. The lower signal of the protein present in the wood might be explained by the lower sensitivity of the antibodies that indeed showed weaker signals also in leaf samples.

Both the ETR values and presence of RuBisCo in the wood corroborate the hypothesis that wood photosynthesis can recycle the CO_2 dissolved in the xylem sap (Alessio et al. 2005, Wittmann et al. 2006, Berveiller and Damesin 2008, Bloemen et al. 2013*a*, 2013*c*, Vandegehuchte et al. 2015).

Recent research has suggested that local production of carbohydrates by bark photosynthesis may facilitate osmotic adjustment to support turgor maintenance and xylem functioning under drought stress (Zwieniecki and Holbrook 2009, Nardini et al. 2011, 2018, Secchi and Zwieniecki 2012, Cernusak and Cheesman 2015, Ávila-Lovera et al. 2017, De Roo et al. 2020, Tomasella et al. 2020). Our data let us speculate that even wood chloroplasts might play a very local role in these processes, especially in post-drought hydraulic recovery, paving the way for future studies on this topic.

Conclusions

In conclusion, our experimental setup enabled us to define in detail the functional features of stem chloroplasts of *F. ornus*, and their potential photosynthetic efficiency. The comparison of the P700 kinetics in different compartments raises interesting questions on the relative amount of linear and cyclic electron flow in the wood. From the current literature, it is known that the presence of chloroplasts and the related photosynthetic activity decrease with increasing stem age. In accordance, we found that the bark of current year stems has a conformation of the photosynthetic apparatus almost comparable to that of the adjacent leaves. Moreover, already in the 1-year-old stem, there is a decrease in ETRs, compatible with decreased light transmittance. In accordance with our expectations, chloroplasts in the wood of different ages showed good photosynthetic efficiency, supporting the idea that stem photosynthesis participates in the production of photosynthates that might support plant carbon balance. This functional feature invites to speculate that stem photosynthesis might play an adaptive advantage, especially for woody plant species occurring in habitats where seasonal drought can strongly limit leaf photosynthesis, which is, in fact, the case for *F. ornus*.

Data availability statement

The data that support the findings of this study are available from the corresponding author upon reasonable request.

Acknowledgments

We are very grateful to the 'Direzione centrale risorse agroalimentari, forestali e ittiche – area foreste e territorio' of the 'Regione Autonoma Friuli Venezia Giulia', and to the public nursery Vivai Pascul (Tarcento, Italy) for providing the plant material for the glasshouse experiment. We thank the Electron Microscopy Facility of the Department of Biology at the University of Padova. Figure S1 available as Supplementary data at *Tree Physiology* Online was created with BioRender.com.

Conflict of interest

None declared.

Authors' contributions

A.N., T.M., A.A., N.L.R. and S.N. designed the experiment; N.L.R., A.A., M.B. and S.N. performed pigments analysis and fluorescence spectroscopy measurements; S.N. and M.B. performed light-transmission measurements and analysis; N.L.R. and S.N. performed epifluorescence microscopy and TEM observations; A.A. and S.N. performed SDS-PAGE electrophoresis and western blot analysis; T.M., A.A. and S.N. contributed to imaging and spectroscopy data acquisition and analyses. S.N. and A.N. wrote the manuscript, with contributions and revisions from all authors.

References

Albanese P, Manfredi M, Meneghesso A, Marengo E, Saracco G, Barber J, Morosinotto T, Pagliano C (2016) Dynamic reorganization of photosystem II supercomplexes in response to variations in light intensities. Biochim Biophys Acta 1857:1651–1660.

Alessio GA, Pietrini F, Brilli F, Loreto F (2005) Characteristics of CO_2 exchange between peach stems and the atmosphere. Funct Plant Biol 32:787–795.

Allorent G, Osorio S, Ly Vu J et al. (2015) Adjustments of embryonic photosynthetic activity modulate seed fitness in *Arabidopsis thaliana*. New Phytol 205:707–719.

Allorent G, Byrdin M, Carraretto L, Morosinotto T, Szabo I, Finazzi G (2018) Global spectroscopic analysis to study the regulation of the photosynthetic proton motive force: A critical reappraisal. Biochim Biophys Acta Bioenerg 1859:676–683.

Anderson JM (1986) Photoregulation of the composition, function, and structure of thylakoid membranes. Annu Rev Plant Physiol 37:93–136.

Anderson JM, Goodchild DJ, Boardman NK (1973) Composition of the photosystems and chloroplast structure in extreme shade plants. Biochim Biophys Acta 325:573–585.

Anderson JM, Chow WS, Park YI (1995) The grand design of photosynthesis: acclimation of the photosynthetic apparatus to environmental cues. Photosynth Res 46:129–139.

Anderson JM, Horton P, Kim EH, Chow WS (2012) Towards elucidation of dynamic structural changes of plant thylakoid architecture. Philos Trans R Soc Lond B Biol Sci 367:3515–3524.

Andrizhiyevskaya EG, Chojnicka A, Bautista JA, Diner BA, van Grondelle R, Dekker JP (2005) Origin of the F685 and F695 fluorescence in photosystem II. Photosynth Res 84:173–180.

Angyalossy V, Pace MR, Evert RF et al. (2016) IAWA list of microscopic bark features. IAWA J 37:517–615.

Aschan G, Pfanz H (2003) Non-foliar photosynthesis–a strategy of additional carbon acquisition. Flora Morphol Distrib Funct Ecol Plants 198:81–97.

Aschan G, Wittmann C, Pfanz H (2001) Age-dependent bark photosynthesis of aspen twigs. Trees 15:431–437.

Ávila E, Herrera A, Tezara W (2014) Contribution of stem CO_2 fixation to whole-plant carbon balance in nonsucculent species. Photosynthetica 52:3–15.

Ávila-Lovera E, Zerpa AJ, Santiago LS (2017) Stem photosynthesis and hydraulics are coordinated in desert plant species. New Phytol 216:1119–1129.

Bailleul B, Cardol P, Breyton C, Finazzi G (2010) Electrochromism: a useful probe to study algal photosynthesis. Photosynth Res 106:179–189.

Ballottari M, Dall'Osto L, Morosinotto T, Bassi R (2007) Contrasting behavior of higher plant photosystem I and II antenna systems during acclimation. J Biol Chem 282:8947–8958.

Berveiller D, Damesin C (2008) Carbon assimilation by tree stems: potential involvement of phosphoenolpyruvate carboxylase. Trees 22:149–157.

Berveiller D, Kierzkowski D, Damesin C (2007) Interspecific variability of stem photosynthesis among tree species. Tree Physiol 27:53–61.

Björkman O, Demmig B (1987) Photon yield of O_2 evolution and chlorophyll fluorescence characteristics at 77 K among vascular plants of diverse origins. Planta 170:489–504.

Bloemen J, McGuire MA, Aubrey DP, Teskey RO, Steppe K (2013*a*) Internal recycling of respired CO_2 may be important for plant functioning under changing climate regimes. Plant Signal Behav 8: e27530.

Bloemen J, McGuire MA, Aubrey DP, Teskey RO, Steppe K (2013*b*) Transport of root-respired CO_2 via the transpiration stream affects aboveground carbon assimilation and CO_2 efflux in trees. New Phytol 197:555–565.

Bloemen J, Overlaet-Michiels L, Steppe K (2013*c*) Understanding plant responses to drought: how important is woody tissue photosynthesis? Acta Hortic 991:149–157.

Bloemen J, Vergeynst L, Overlaet-Michiels L, Steppe K (2016) How important is woody tissue photosynthesis in poplar during drought stress? Trees 30:63–72.

Breton J (1982) The 695 nm fluorescence (F 695) of chloroplasts at low temperature is emitted from the primary acceptor of photosystem II. FEBS Lett 147:16–20.

Brugnoli E, Cona A, Lauteri M (1994) Xanthophyll cycle components and capacity for non-radiative energy dissipation in sun and shade leaves of *Ligustrum ovalifolium* exposed to conditions limiting photosynthesis. Photosynth Res 41:451–463.

Cernusak LA, Cheesman AW (2015) The benefits of recycling: how photosynthetic bark can increase drought tolerance. New Phytol 208:995–997.

Cernusak LA, Hutley LB (2011) Stable isotopes reveal the contribution of corticular photosynthesis to growth in branches of *Eucalyptus miniata*. Plant Physiol 155:515–523.

Cernusak LA, Marshall JD (2000) Photosynthetic refixation in branches of Western White Pine. Funct Ecol 14:300–311.

Cernusak LA, Marshall JD, Comstock JP, Balster NJ (2001) Carbon isotope discrimination in photosynthetic bark. Oecologia 128:24–35.

Chow WS, Melis A, Anderson J (1990) Adjustments of photosystem stoichiometry in chloroplasts improve the quantum efficiency of photosynthesis. Proc Natl Acad Sci USA 87:7502–7506.

Comstock J, Ehleringer J (1990) Effect of variations in leaf size on morphology and photosynthetic rate of twigs. Funct Ecol 4: 209–221.

Damesin C (2003) Respiration and photosynthesis characteristics of current-year stems of *Fagus sylvatica*: from the seasonal pattern to an annual balance. New Phytol 158:465–475.

De Baerdemaeker NJ, Salomón RL, De Roo L, Steppe K (2017) Sugars from woody tissue photosynthesis reduce xylem vulnerability to cavitation. New Phytol 216:720–727.

De Roo L, Salomón RL, Steppe K (2020) Woody tissue photosynthesis reduces stem CO_2 efflux by half and remains unaffected by drought stress in young *Populus tremula* trees. Plant Cell Environ 43: 981–991.

Dobrev K, Stanoeva D, Velitchkova M, Popova AV (2016) The lack of lutein accelerates the extent of light-induced bleaching of photosynthetic pigments in thylakoid membranes of *Arabidopsis thaliana*. Photochem Photobiol 92:436–445.

Dymova O, Khristin M, Miszalski Z, Kornas A, Strzalka K, Golovko T (2018) Seasonal variations of leaf chlorophyll-protein complexes in the wintergreen herbaceous plant *Ajuga reptans* L. Funct Plant Biol 45:519–527.

Eberhard S, Finazzi G, Wollman FA (2008) The dynamics of photosynthesis. Annu Rev Genet 42:463–515.

Filippou M, Fasseas C, Karabourniotis G (2007) Photosynthetic characteristics of olive tree (*Olea europaea*) bark. Tree Physiol 27:977–984.

Flannery SE, Hepworth C, Wood WH, Pastorelli F, Hunter CN, Dickman MJ, Jackson PJ, Johnson MP (2021) Developmental acclimation of the thylakoid proteome to light intensity in *Arabidopsis*. Plant J 105:223–244.

Gerotto C, Alboresi A, Meneghesso A, Jokel M, Suorsa M, Aro EM, Morosinotto T (2016) Flavodiiron proteins act as safety valve for electrons in *Physcomitrella patens*. Proc Natl Acad Sci USA 113:12322–12327.

Gibson A (1983) Anatomy of photosynthetic old stems of nonsucculent dicotyledons from North American deserts. Bot Gaz 144: 347–362.

Gortan E, Nardini A, Gascó A, Salleo S (2009) The hydraulic conductance of *Fraxinus ornus* leaves is constrained by soil water availability and coordinated with gas exchange rates. Tree Physiol 29:529–539.
Govindjee (1995) Sixty-three years since Kautsky: chlorophyll a fluorescence. Aust J Plant Physiol 22:131–160.
Grieco M, Suorsa M, Jajoo A, Tikkanen M, Aro EM (2015) Light-harvesting II antenna trimers connect energetically the entire photosynthetic machinery—including both photosystems II and I. Biochim Biophys Acta 1847:607–619.
Hibberd JM, Quick WP (2002) Characteristics of C4 photosynthesis in stems and petioles of C3 flowering plants. Nature 415:451–454.
Hu C, Nawrocki WJ, Croce R (2021) Long-term adaptation of *Arabidopsis thaliana* to far-red light. Plant Cell Environ 44:3002–3014.
Ivanov AG, Ignatova NS, Christov AM (1990) Comparative ultrastructural and fluorescence studies of grapevine (*Vitis vinifera* L.) chloroplasts isolated from stem and leaf tissues. Plant Sci 67:253–257.
Ivanov AG, Krol M, Sveshnikov D, Malmberg G, Gardeström P, Hurry V, Öquist G, Huner NPA (2006) Characterization of the photosynthetic apparatus in cortical bark chlorenchyma of Scots pine. Planta 223:1165–1177.
Ke B (1972) The rise time of photoreduction, difference spectrum, and oxidation-reduction potential of P430. Arch Biochem Biophys 152:70–77.
Kharouk VI, Middleton EM, Spencer SL, Rock BN, Williams DL (1995) Aspen bark photosynthesis and its significance to remote sensing and carbon budget estimates in the boreal ecosystem. Water Air Soil Pollut 82:483–497.
Krause GH, Weis E (1984) Chlorophyll fluorescence as a tool in plant physiology II. Interpretation of fluorescence signals. Photosynth Res 5:139–157.
Krause GH, Weis E (1991) Chlorophyll fluorescence and photosynthesis—the basics. Annu Rev Plant Physiol Plant Mol Biol 42:313–349.
La Rocca N, Sciuto K, Meneghesso A, Moro I, Rascio N, Morosinotto T (2015) Photosynthesis in extreme environments: responses to different light regimes in the Antarctic alga *Koliella antarctica*. Physiol Plant 153:654–667.
Lamb J, Forfang K, Hohmann-Marriott M (2015) A practical solution for 77 K fluorescence measurements based on LED excitation and CCD array detector. PLoS One 10:e0132258.
Lamb JJ, Røkke G, Hohmann-Marriott MF (2018) Chlorophyll fluorescence emission spectroscopy of oxygenic organisms at 77 K. Photosynthetica 56:105–124.
Larcher W, Lütz C, Nagele M, Bodner M (1988) Photosynthetic functioning and ultrastructure of chloroplasts in stem tissues of *Fagus sylvatica*. J Plant Physiol 132:731–737.
Lee WJ, Whitmarsh J (1989) Photosynthetic apparatus of pea thylakoid membranes: response to growth light intensity. Plant Physiol 89:932–940.
Lemeille S, Rochaix JD (2010) State transitions at the crossroad of thylakoid signalling pathways. Photosynth Res 106:33–46.
Lichtenthaler HK, Buschmann C, Döll M, Fietz HJ, Bach T, Kozel U, Meier D, Rahmsdorf U (1981) Photosynthetic activity, chloroplast ultrastructure, and leaf characteristics of high-light and low-light plants and of sun and shade leaves. Photosynth Res 2:115–141.
Lichtenthaler HK, Babani F, Navrátil M, Buschmann C (2013) Chlorophyll fluorescence kinetics, photosynthetic activity, and pigment composition of blue-shade and half-shade leaves as compared to sun and shade leaves of different trees. Photosynth Res 117:355–366.
Liu J, Gu L, Yu Y, Huang P, Wu Z, Zhang Q, Qian Y, Wan X, Sun Z (2019) Corticular photosynthesis drives bark water uptake to refill embolized vessels in dehydrated branches of *Salix matsudana*. Plant Cell Environ 42:2584–2596.
Liu J, Sun C, Zhai FF, Li Z, Qian Y, Gu L, Sun Z (2021) Proteomic insights into the photosynthetic divergence between bark and leaf chloroplasts in *Salix matsudana*. Tree Physiol 41: 2142–2152.
Manetas Y (2004) Probing corticular photosynthesis through in vivo chlorophyll fluorescence measurements: evidence that high internal CO_2 levels suppress electron flow and increase the risk of photoinhibition. Physiol Plant 120:509–517.
Manetas Y, Pfanz H (2005) Spatial heterogeneity of light penetration through periderm and lenticels and concomitant patchy acclimation of corticular photosynthesis. Trees 19:409–414.
Maxwell K, Johnson GN (2000) Chlorophyll fluorescence—a practical guide. J Exp Bot 51:659–668.
Mazur R, Mostowska A, Kowalewska Ł (2021) How to measure grana–ultrastructural features of thylakoid membranes of plant chloroplasts. Front Plant Sci 12:756009.
Melis A, Harvey GW (1981) Regulation of photosystem stoichiometry, chlorophyll-a and chlorophyll-B content and relation to chloroplast ultrastructure. Biochim Biophys Acta 637:138–145.
Mellon M, Storti M, Vera-Vives AM, Kramer DM, Alboresi A, Morosinotto T (2021) Inactivation of mitochondrial complex I stimulates chloroplast ATPase in *Physcomitrium patens*. Plant Physiol 187: 931–946.
Minagawa J (2011) State transitions—the molecular remodeling of photosynthetic supercomplexes that controls energy flow in the chloroplast. Biochim Biophys Acta 1807:897–905.
Morosinotto T, Breton J, Bassi R, Croce R (2003) The nature of a chlorophyll ligand in Lhca proteins determines the far red fluorescence emission typical of photosystem I. J Biol Chem 278:49223–49229.
Mukherjee A (2020) State transition regulation in *Chlamydomonas reinhardtii*. Plant Physiol 183:1418–1419.
Murchie EH, Horton P (1997) Acclimation of photosynthesis to irradiance and spectral quality in British plant species: chlorophyll content, photosynthetic capacity and habitat preference. Plant Cell Environ 20:438–448.
Nardini A, Salleo S, Trifilò P, Lo Gullo MA (2003) Water relations and hydraulic characteristics of three woody species co-occurring in the same habitat. Ann For Sci 60:297–305.
Nardini A, Lo Gullo MA, Salleo S (2011) Refilling embolized xylem conduits. Is it a matter of phloem unloading? Plant Sci 180: 604–611.
Nardini A, Savi T, Trifilò P, Lo Gullo MA (2018) Drought stress and the recovery from xylem embolism in woody plants. In: Cánovas FM, Luettge U, Matyssek R (eds) Progress in botany. Springer, Berlin, Germany, pp 137–231.
Nardini A, Petruzzellis F, Marusig D et al. (2021) Water 'on the rocks': a summer drink for thirsty trees? New Phytol 229:199–212.
Nilsen ET (1995) Stem photosynthesis: extent, patterns and role in plant carbon economy. In: Gartner B (ed) Plant stems: physiology and functional morphology. Academic Press, San Diego, CA, USA, pp 223–240.
Nilsen ET, Sharifi MR (1994) Seasonal acclimation of stem photosynthesis in woody legume species from the Mojave and Sonoran deserts of California. Plant Physiol 105:1385–1391.
Pfanz H (2008) Bark photosynthesis. Trees 22:137–138.
Pfanz H, Aschan G (2001) The existence of bark and stem photosynthesis in woody plants and its significance for the overall carbon gain. An eco-physiological and ecological approach. Prog Bot 62: 477–510.
Pfanz H, Aschan G, Langenfeld-Heyser R, Wittmann C, Loose M (2002) Ecology and ecophysiology of tree stems: corticular and wood photosynthesis. Naturwissenschaften 89:147–162.
Pilarski J (1989) Optical properties of bark and leaves of *Syringa vulgaris* L. Bull Pol Acad Sci Biol Sci 37:253–260.
Pilarski J (1999) Gradient of photosynthetic pigments in the bark and leaves of lilac (*Syringa vulgaris* L.). Acta Physiol Plant 21:365–373.

R Core Team (2021) R: A language and environment for statistical computing. R Foundation for Statistical Computing, Vienna, Austria. https://www.R-project.org/.

Ruban AV, Johnson MP (2009) Dynamics of higher plant photosystem cross-section associated with state transitions. Photosynth Res 99:173–183.

Sacksteder CA, Kramer DM (2000) Dark-interval relaxation kinetics (DIRK) of absorbance changes as a quantitative probe of steady-state electron transfer. Photosynth Res 66:145–158.

Saveyn A, Steppe K, Ubierna N, Dawson TE (2010) Woody tissue photosynthesis and its contribution to trunk growth and bud development in young plants. Plant Cell Environ 33:1949–1958.

Schaedle M (1975) Tree photosynthesis. Annu Rev Plant Physiol 26:101–115.

Schmitz N, Egerton JJG, Lovelock CE, Ball MC (2012) Light-dependent maintenance of hydraulic function in mangrove branches: do xylary chloroplasts play a role in embolism repair? New Phytol 195:40–46.

Secchi F, Zwieniecki MA (2011) Sensing embolism in xylem vessels: the role of sucrose as a trigger for refilling. Plant Cell Environ 34:514–524.

Secchi F, Zwieniecki MA (2012) Analysis of xylem sap from functional (nonembolized) and nonfunctional (embolized) vessels of *Populus nigra*: chemistry of refilling. Plant Physiol 160:955–964.

Secchi F, Pagliarani C, Cavalletto S et al. (2021) Chemical inhibition of xylem cellular activity impedes the removal of drought- induced embolisms in poplar stems - new insights from micro-CT analysis. New Phytol 229:820–830.

Solhaug KA, Gauslaa Y, Haugen J (1995) Adverse effects of epiphytic crustose lichens upon stem photosynthesis and chlorophyll of *Populus tremula* L. Bot Acta 108:233–239.

Steppe K, Sterck F, Deslauriers A (2015) Diel growth dynamics in tree stems: linking anatomy and ecophysiology. Trends Plant Sci 20:335–343.

Storti M, Segalla A, Mellon M, Alboresi A, Morosinotto T (2020) Regulation of electron transport is essential for photosystem I stability and plant growth. New Phytol 228:1316–1326.

Sun Q, Kiyotsugu Y, Mitsuo S, Hitoshi S (2003) Vascular tissue in the stem and roots of woody plants can conduct light. J Exp Bot 54:1627–1635.

Sun Q, Yoda K, Suzuki H (2005) Internal axial light conduction in the stems and roots of herbaceous plants. J Exp Bot 56: 191–203.

Tausz M, Warren CR, Adams MA (2005) Is the bark of shining gum (*Eucalyptus nitens*) a sun or a shade leaf? Trees 19:415–421.

Teskey RO, Saveyn A, Steppe K, McGuire MA (2008) Origin, fate and significance of CO_2 in tree stems. New Phytol 177:17–32.

Tomasella M, Petrussa E, Petruzzellis F, Nardini A, Casolo V (2020) The possible role of non-structural carbohydrates in the regulation of tree hydraulics. Int J Mol Sci 21:144.

Trifilò P, Natale S, Gargiulo S, Abate E, Casolo V, Nardini A (2021) Stem photosynthesis affects hydraulic resilience in the deciduous *Populus alba* but not in the evergreen *Laurus nobilis*. Water 13:2911.

van Cleve B, Forreiter C, Sauter JJ, Apel K (1993) Pith cells of poplar contain photosynthetically active chloroplasts. Planta 189:70–73.

Vandegehuchte MW, Bloemen J, Vergeynst LL, Steppe K (2015) Woody tissue photosynthesis in trees: salve on the wounds of drought? New Phytol 208:998–1002.

Wellburn AR (1994) The spectral determination of chlorophylls a and b, as well as total carotenoids, using various solvents with spectrophotometers of different resolution. J Plant Physiol 144:307–313.

Wiebe HH (1975) Photosynthesis in wood. Physiol Plant 33:245–246.

Wientjes E, van Amerongen H, Croce R (2013) LHCII is an antenna of both photosystems after long-term acclimation. Biochim Biophys Acta 1827:420–426.

Witt HT (1979) Energy conversion in the functional membrane of photosynthesis. Analysis by light pulse and electric pulse methods. The central role of the electric field. Biochim Biophys Acta 505:355–427.

Wittmann C, Pfanz H (2007) Temperature dependency of bark photosynthesis in beech (*Fagus sylvatica* L.) and birch (*Betula pendula* Roth.) trees. J Exp Bot 58:4293–4306.

Wittmann C, Pfanz H (2008) General trait relationships in stems: a study on the performance and interrelationships of several functional and structural parameters involved in corticular photosynthesis. Physiol Plant 134:636–648.

Wittmann C, Pfanz H (2014) Bark and woody tissue photosynthesis: a means to avoid hypoxia or anoxia in developing stem tissues. Funct Plant Biol 41:940–953.

Wittmann C, Pfanz H (2016) The optical, absorptive and chlorophyll fluorescence properties of young stems of five woody species. Environ Exp Bot 121:83–93.

Wittmann C, Aschan G, Pfanz H (2001) Leaf and twig photosynthesis of young beech (*Fagus sylvatica*) and aspen (*Populus tremula*) trees grown under different light intensity regimes. Basic Appl Ecol 2:145–154.

Wittmann C, Pfanz H, Pietrini F (2005) Light-modulation of corticular CO_2-refixation in young birch stems (*Betula pendula* Roth.). Phyton-Ann Rei Bot 45:195–212.

Wittmann C, Pfanz H, Loreto F, Centritto M, Pietrini F, Alessio G (2006) Stem CO_2 release under illumination: corticular photosynthesis, photorespiration or inhibition of mitochondrial respiration? Plant Cell Environ 29:1149–1158.

Zwieniecki MA, Holbrook NM (2009) Confronting Maxwell's demon: biophysics of xylem embolism repair. Trends Plant Sci 14:530–534.